npj | climate and atmospheric science

www.nature.com/npjclimatsci

ARTICLE OPEN

The role of future anthropogenic methane emissions in air quality and climate

Zosia Staniaszek[1]✉, Paul T. Griffiths[1,2], Gerd A. Folberth[3], Fiona M. O'Connor[3], N. Luke Abraham[1,2] and Alexander T. Archibald[1,2]✉

Mitigation of greenhouse gas emissions is crucial for achieving the goals of the Paris climate agreement. One key gas is methane, whose representation in most climate models is limited by using prescribed surface concentrations. Here we use a new, methane emissions-driven version of the UK Earth System Model (UKESM1) and simulate a zero anthropogenic methane emissions scenario (ZAME) in order to (i) attribute the role of anthropogenic methane emissions on the Earth system and (ii) bracket the potential for theoretical maximum mitigation. We find profound, rapid and sustained impacts on atmospheric composition and climate, compared to a counterfactual projection (SSP3-7.0, the 'worst case' scenario for methane). In ZAME, methane declines to below pre-industrial levels within 12 years and global surface ozone decreases to levels seen in the 1970s. By 2050, 690,000 premature deaths per year and 1° of warming can be attributed to anthropogenic methane in SSP3-7.0. This work demonstrates the significant maximum potential of methane emissions reductions, and their air-quality co-benefits, but also reiterates the need for action on carbon dioxide (CO_2) emissions. We show that a methane emissions-driven treatment is essential for simulating the full Earth system impacts and feedbacks of methane emissions changes.

npj Climate and Atmospheric Science (2022)5:21 ; https://doi.org/10.1038/s41612-022-00247-5

INTRODUCTION

In order to achieve the Paris agreement goals[1], many countries are committing to reducing greenhouse gas (GHG) emissions to net-zero by 2050 (see https://eciu.net/netzerotracker). Carbon dioxide (CO_2) mitigation is fundamental to minimise long-term temperature increase, and the peak global warming is proportional to the cumulative CO_2 emissions. Near-term climate forcers (NTCFs) including methane, ozone (O_3) and aerosols, have much shorter lifetimes than CO_2, and provide opportunities for short-term mitigation. Unlike for CO_2, their climate forcing is determined by the rate of emissions[2].

Methane (CH_4) is a potent GHG but has a short lifetime compared with CO_2 (9.1 ± 0.9 years, total atmospheric lifetime[3]), mainly due to its reaction with the hydroxyl radical (OH). Since pre-industrial times, anthropogenic methane emissions have caused more than a doubling of the abundance of methane in the atmosphere, with rapid growth in recent years[4], and especially in 2020 (gml.noaa.gov/ccgg/trends_ch4/). These emissions now make up 60% of the total methane source and come from fossil fuel use, agriculture and waste management[5].

The role of methane as a lever to achieve climate goals is an active topic[6–9]. Over 100 countries (representing 50% of anthropogenic methane emissions) recently signed up to the Global Methane Pledge (globalmethanepledge.org), and there is extensive potential for mitigation[8,10,11]. This includes reduction of hot-spot emissions (such as gas leakage and waste management, e.g. Höglund-Isaksson et al.[12]) and direct air capture[13,14]. Ocko et al.[7] found that a quarter of a degree of warming could be avoided by 2050 by implementing currently available methane mitigation technologies. This paper assesses the impacts of methane emissions on the Earth system by exploring a zero anthropogenic methane emissions scenario (ZAME).

Previous studies (e.g. refs. [8,15–18]) have highlighted the significant co-benefits of methane mitigation for climate on global air quality, principally through tropospheric ozone. Recently, Allen et al.[17] used Shared Socioeconomic Pathway (SSP) experiments from the Aerosol and Chemistry Model Intercomparison Project (AerChemMIP) to isolate the methane-only contribution of NTCF mitigation from a high methane scenario (SSP3-7.0) level down to SSP1-2.6 levels. In this study, they show that by 2050, the global mean atmospheric methane concentration decreases by 26%, resulting in a 9.7% decrease in surface ozone concentrations, and a temperature decrease of 0.39 ± 0.05 K, compared to SSP3-7.0. Shindell et al.[8] explored a methane concentration reduction of 30% compared to the present day (2015) using an ensemble of models. They attributed a global population-weighted ozone exposure decrease of 2–2.5 ppb, and a temperature decrease of 0.18 ± 0.02 K to the methane change.

Whilst simpler climate models (e.g. Hayman et al.[19]) can be used to rapidly assess the surface temperature effects of different emissions scenarios, their interactive modelling of methane processes, particularly the effects of methane on tropospheric oxidising capacity, are limited. On the other hand, general circulation models (GCMs) and Earth system models (ESMs) are able to represent the atmospheric processes involving methane more fully. Traditionally, these complex models use a methane lower boundary condition (LBC): a global time-varying methane surface concentration pre-calculated from emissions. This leads to a buffering effect at the surface, which limits the feedback of atmospheric oxidation on methane levels[20]. The new emissions-driven configuration of the UK Chemistry and Aerosol model (UKCA), coupled to UKESM1.0 (hereafter referred to as UKCA-CH4[21], (GAF, ZS, ATA, PTG, FOC et al. 2022, submitted for publication) allows us to bridge the benefits of these two

[1]Centre for Atmospheric Science, Department of Chemistry, University of Cambridge, Cambridge, UK. [2]National Centre for Atmospheric Science, Department of Chemistry, University of Cambridge, Cambridge, UK. [3]Met Office Hadley Centre, Exeter, UK. ✉email: znjs2@cam.ac.uk; ata27@cam.ac.uk

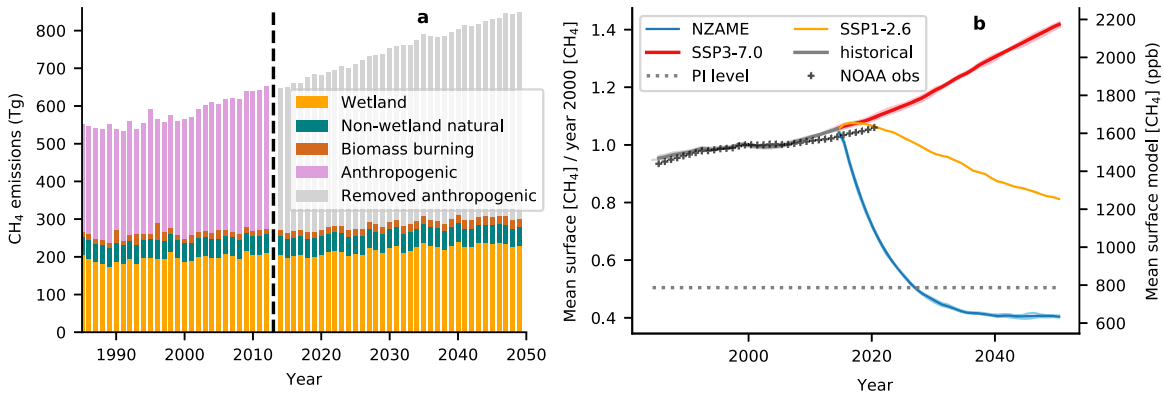

Fig. 1 Methane emissions inputs and the resulting surface methane concentrations in UKCA-CH4. a Methane emissions used as inputs into UKCA-CH4 for 1985–2050, from Gidden et al.[23]. The emissions are split into sectors: interactive wetland emissions (orange), non-wetland natural (green), biomass burning (dark orange), anthropogenic (pink) and removed anthropogenic in the zero anthropogenic methane emissions scenario (ZAME, grey). **b** Methane surface concentrations from 1985 to 2050 relative to the year 2000 (left-hand *y* axis). The right-hand *y* axis shows the corresponding modelled absolute methane concentration. Historical model concentrations are in dark grey and observations (Dlugokencky, NOAA/GML (gml.noaa.gov/ccgg/trends_ch4/) are shown by crosses. Three future scenarios are shown: ZAME (blue), SSP3-7.0 (red) and SSP1-2.6 (orange). The pre-industrial (PI) level is shown by the dotted line. The fainter coloured lines show the three individual ensemble members and the darker line shows the ensemble mean, for SSP3-7.0 and ZAME.

approaches. Previously Shindell et al.[18] used an emissions-driven configuration of the GISS GCM to model methane increases from pre-industrial to the present day. More recently, He et al.[22] have also developed a methane emissions-driven version of the Geophysical Fluid Dynamics Laboratory Atmospheric Model (GFDL AM4.1), and replicated the historic period by optimising the methane emissions. UKCA-CH4 goes further by using emissions inputs from inventories[23] and interactive (instead of climatological) wetland emissions (see 'Methods'). As a result, we are now able to simulate the effects of zero anthropogenic methane emissions within a fully interactive Earth system model.

Abernethy et al.[24] also used UKCA-CH4 in a recent study focused on methane removal scenarios, with different removal amounts and rates. By sampling the scenario space, they defined methane–climate and methane–ozone response metrics for measuring the effectiveness of different removal trajectories. Methane affects ozone via its interaction with HOx radials (=OH and HO_2), which propagate NOx (=NO and NO_2) interconversion[25]. Through methane, HOx and NOx are closely coupled.

In this study, we explore the role of anthropogenic methane in the Earth system in a future climate scenario. Our underlying, or counterfactual scenario is SSP3-7.0: the most extreme future methane trajectory in the Sixth Coupled Model Intercomparison Project (CMIP6) [23], but one that closely matches the recent trends in methane observations (see Fig. 1b). To simulate the effects of zero anthropogenic methane, we instantaneously removed all of the anthropogenic methane emissions from SSP3-7.0, from 2015 to 2050. This scenario is hereafter referred to as ZAME. We examine these methane emissions reductions not as a feasible strategy, but to show the effect of anthropogenic methane in the counterfactual SSP3-7.0 scenario via the impacts of maximum theoretical emission mitigation. We aim to highlight the importance of limiting further methane increases and the significant maximum potential of emissions reductions.

RESULTS

The impacts of ZAME on atmospheric composition

In the ZAME scenario, (following the cessation of anthropogenic methane emissions, Fig. 1a), surface methane decreases globally with an e-folding timescale of 6.55 ± 0.06 years, and reaches below pre-industrial levels by 2030 (i.e. within 15 years; see Fig. 1b). The whole atmosphere methane burden declines to below pre-industrial levels within 12 years, stabilising at 1775 ± 15 Tg, 71% below the counterfactual in 2050.

Commensurate with the decrease in methane, levels of OH increase. OH is the main component of the atmosphere's oxidising capacity, and determines the methane lifetime, but itself is controlled by the amount of methane and other reactive gases in the atmosphere[26]. The magnitude of the OH sink decreases in ZAME due to the changes in methane: directly via reduction of the $CH_4 + OH$ reaction, and indirectly due to decreases in secondary production of carbon monoxide (CO), the other major OH sink. As a result, the global mean surface OH concentration increases over time in ZAME (see Fig. 2a). It reaches a new constant level of $1.34 \pm 0.01 \times 10^6$ molec cm^{-3} by 2035 (after 20 years), more than 30% higher than the present-day period. This represents a change unprecedented over the historic period (1850–2014)[27] and drives the rapid decrease in the lifetime of methane.

Methane is an important precursor for tropospheric ozone[15]. This relationship holds well in our ZAME scenario: tropospheric ozone is significantly reduced, globally. In SSP3-7.0, population-weighted surface ozone concentration increases linearly from 2015 to 2050, reaching 35.32 ± 0.07 ppb (9.4% higher than 2014, Fig. 2d). In ZAME, the surface ozone concentration decreases rapidly in the first decade, then stabilises to a new steady-state value of 27.8 ± 0.5 ppb (13.9% below 2014) up to 2050. This corresponds to historical global population-weighted ozone levels from the 1970s (simulated with UKESM1.0). The population data used are consistent between the simulations (from SSP3[28]), so the differences stem from the regional surface ozone changes.

In SSP3-7.0, the area-weighted surface ozone concentration remains constant over the time period of the experiment. However, the population-weighted concentration increases (Fig. 2d), showing that the proportion of the population living in high-ozone areas increases in the counterfactual. In ZAME, both the population-weighted and the area-weighted ozone concentrations decrease.

The largest ozone reductions in ZAME occur in the Northern Hemisphere tropics (see Fig. 2c), in regions associated with the highest tropospheric ozone precursor emissions[25,29]. These are populous regions, such as over India, implying methane emissions have an important role on air quality and human health in these regions.

To quantify the air-quality impacts of anthropogenic methane, we calculated the long-term ozone-related mortality for SSP3-7.0 and ZAME for 2050, according to the method in Malley et al.[30]. We found

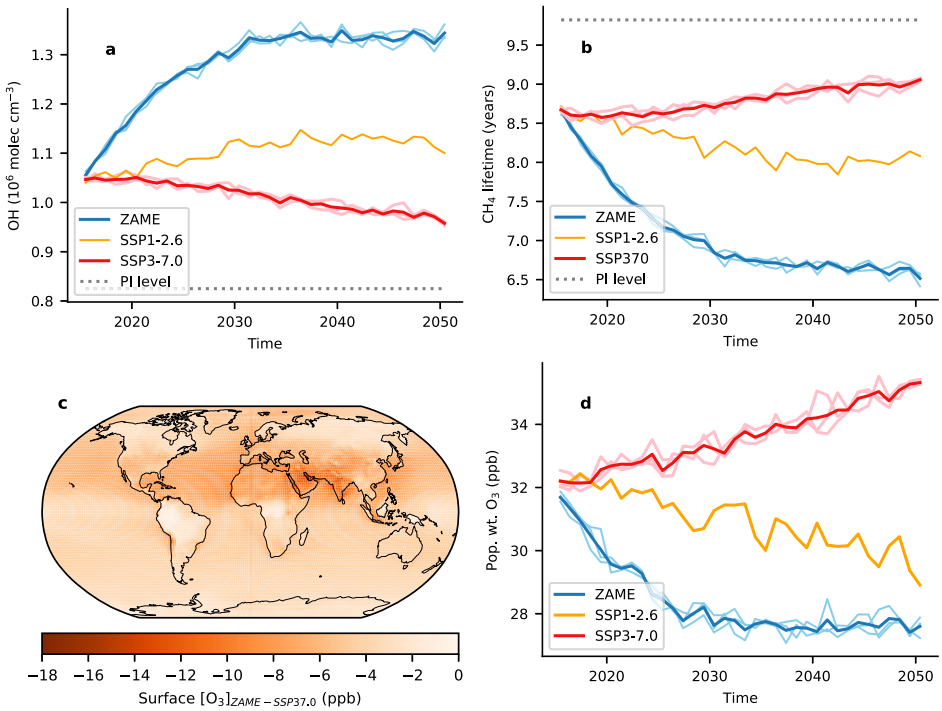

Fig. 2 Atmospheric composition changes over time in the zero anthropogenic methane scenario (ZAME) from 2015 to 2050. The SSP3-7.0 scenario is shown in red, ZAME in blue, SSP1-2.6 in orange and pre-industrial values in dotted grey. The fainter coloured lines show the three individual ensemble members and the darker line shows the ensemble mean, for SSP3-7.0 and ZAME. **a** Global mean (airmass-weighted) tropospheric OH concentration. **b** Methane lifetime, defined as total atmosphere burden divided by CH_4-OH flux in the troposphere. **c** Decadal mean (2040–2050) change in surface ozone concentrations in ZAME compared to SSP3-7.0. **d** Population-weighted surface ozone concentration. Population datasets are based on the underlying SSP scenarios[46]. The tropopause is defined as a $[O_3] = 125$ ppb surface.

that the ozone associated with anthropogenic methane is responsible for 690,000 premature deaths per year (456,000–910,000, lower and upper bounds of mortality rate) in 2050: 43% from respiratory causes and 57% from cardiovascular causes. This corresponds to around 1270 annual deaths per million tonnes (Tg) of methane emissions, or 65% higher total (ozone-related) deaths per year compared to ZAME. This figure is lower than the results from the recent Global Methane Assessment (GMA) report[8] (~1400 fewer deaths per Tg CH_4 mitigated). This may be due to the use of global average instead of country-specific mortality (see 'Methods'), which is likely to lead to an underestimate in deaths attributed to methane via ozone. However, the air-quality impacts as predicted by UKCA-CH4 are consistent with those from LBC models, and emphasise the opportunities for action on air quality via methane mitigation.

The ozone response to decreased future methane emissions is highly dependent on the underlying scenario. Up to 2050 and beyond, SSP3-7.0 has high emissions of CO, nitrogen oxides (NOx), and volatile organic compounds (VOCs), all of which are precursors for ozone formation. At the opposite end of the spectrum, CO, NOx and VOC emissions decrease substantially in SSP1-2.6[23]. Therefore, anthropogenic methane emissions (reductions) in SSP1-2.6 would have a different impact on ozone. Up to 2050, ZAME gives greater ozone decreases than SSP1-2.6 (see Fig. 2d): the large decrease in methane counteracts the much higher ozone precursor emissions. While the ZAME ozone trend stabilises in the mid 21st century, the ozone in SSP1-2.6 continues to decrease, highlighting the importance of multiple ozone precursor decreases.

The impacts of ZAME on climate

The global mean surface temperature (GMST) increase is substantially reduced in ZAME, compared with the counterfactual—in good agreement with other studies[8,17], and in spite of no change to CO_2. The GMST diverges from the SSP3-7.0 trajectory within a decade of zero anthropogenic methane emissions. Over a 10-20 year time horizon (near-term), the reduction in methane and its indirect effects[31] counterbalance other climate forcers (such as carbon dioxide), so overall there is little temperature change. While the methane concentration stabilises, the other greenhouse gas concentrations continue to increase, leading to increasing temperature after 2035. Over a 20+ year time horizon (the long-term), we see a sustained reduction in the rate of temperature increase: 0.045 (0.036–0.059) K per year in 2035–2050 in ZAME compared to 0.059 (0.055–0.063) K per year in the counterfactual.

By 2050, anthropogenic methane in SSP3-7.0 causes 0.96 ± 0.09 K more warming compared to ZAME (Fig. 3a). Considering the 2040–2050 period (Fig. 3b), the temperature increase is globally uniform, except for in the Arctic, where Arctic amplification is seen in SSP3-7.0. This highlights that anthropogenic methane has the greatest impact in some of the most susceptible regions. The processes contributing to the amplification include feedbacks related to sea ice change, and ocean and atmospheric heat transport[3]—ESMs such as UKCA-CH4 enable these to be simulated.

Between 2015 to 2050 alone, SSP3-7.0 leads to almost 2° of warming in UKCA-CH4 (see Fig. 3a)—the entirety of the temperature limit compared to pre-industrial levels set in the Paris agreement[1]. The total temperature increase (pre-industrial to 2050) in SSP3-7.0 is 2.82 ± 0.12 K. The ZAME experiment shows that 1° of this warming (or one-third of the SSP3-7.0 total temperature increase to 2050) can be attributed to the effects of future anthropogenic methane emissions. This further highlights the potential of methane emissions reductions for climate mitigation[6–8,32] but shows that even the zero methane scenario breaches 1.5°, and underscores the necessity of CO_2 mitigation.

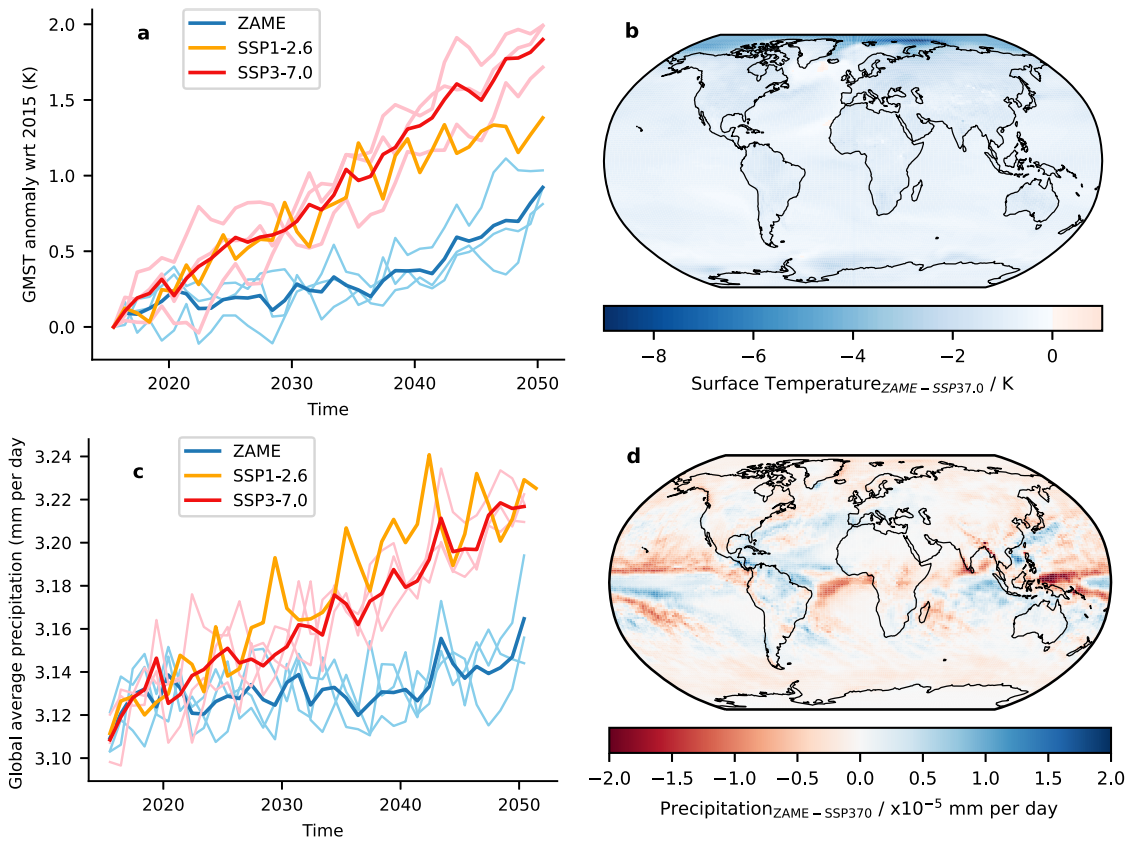

Fig. 3 Physical climate changes associated with zero anthropogenic methane (ZAME), compared to SSP3-7.0 and SSP1-2.6. ZAME is shown in blue, SSP3-7.0 in red and SSP1-2.6 in orange. The fainter coloured lines show the three individual ensemble members and the darker line shows the ensemble mean, for SSP3-7.0 and ZAME. **a** Global mean surface temperature (GMST) anomaly with respect to 2015 values, for 2015–2050. **b** Global surface temperature difference for 2040–2050: ZAME - SSP3-7.0. **c** Global mean precipitation for 2015–2050. **d** 2040–2050 decadal average precipitation in ZAME compared to SSP3-7.0. Red areas correspond to where there is less precipitation in ZAME than SSP3-7.0.

Mirroring the changes in global temperature, removing anthropogenic methane emissions results in a decrease in total precipitation by 2050, and a slowed rate of increase in precipitation compared to the counterfactual (Fig. 3c). By 2040–2050, ZAME results in a small but statistically significant reduction in the rate of precipitation (globally averaged) of 0.061 ± 0.013 mm per day, or 1.9% less. Unlike surface temperature, the spatial distribution of precipitation change is non-uniform, as shown in Fig. 3d. The largest changes occur in the tropics, in the Maritime Continent, a region of greatest precipitation in UKESM1.0 and observations[33].

Comparison with AerChemMIP

Use of a methane emissions-driven configuration may cause a difference in the model's temperature sensitivity with respect to methane (the level of warming for a change in mixing ratio). We analysed the global mean surface temperature sensitivity to methane concentration changes, using the $\Delta\sqrt{[CH_4]}$ relationship from Etminan et al.[34]. We compared our results to the work of Allen et al.[17], who analysed a similar pair of AerChemMIP model experiments based on the SSP3-7.0 scenario. Unlike ZAME, these experiments were based on models using methane lower boundary conditions, and simulated smaller methane reductions. As expected, the GMST response to methane emissions is larger in ZAME than in the AerChemMIP simulations, as shown in Fig. 4a. The response in ZAME (orange cross in Fig. 4a) is also greater than would be expected based on extrapolation of the AerChemMIP multi-model ensemble (MME) results (blue shaded area in Fig. 4a). However, our ZAME results are consistent with an extrapolation of the UKESM1.0 experiment in Allen et al.[17] (green cross and dotted line in Fig. 4a). This most likely reflects a higher sensitivity of GMST to CH_4 in the underlying UKESM1.0 model compared to the AerChemMIP MME, rather than a GMST sensitivity difference between the LBC and emissions-driven model configurations. This is consistent with O'Connor et al.[31], who found a higher present-day effective radiative forcing for methane in UKESM1.0 than in other models considered, which is expected to correlate to a larger GMST response.

Figure 4b compares the ozone response in our ZAME scenario with the AerChemMIP MME. As with GMST, the ZAME simulation represents a greater reduction in O_3 than in the AerChemMIP study. As before, we compared our results (orange cross in Fig. 4b) with the extrapolation of the MME relationship ($\Delta[O_3]/\Delta[CH_4]$), and the UKESM1.0 simulation that was used in deriving the MME relationship (green cross in Fig. 4b). Although there is more variability in the AerChemMIP MME relationship for $\Delta[O_3]/\Delta[CH_4]$ than $\Delta GMST/\Delta[CH_4]$, the results from our ZAME simulation are a clear outlier, compared with both the MME and extrapolation of the UKESM1 simulations. This could be due to extrapolation of the large change in emissions resulting in a non-linear response, but previous work with similar magnitude changes has shown that the $\Delta[O_3]/\Delta[CH_4]$ is linear[15]. We hypothesise that our result is driven by our use of CH_4

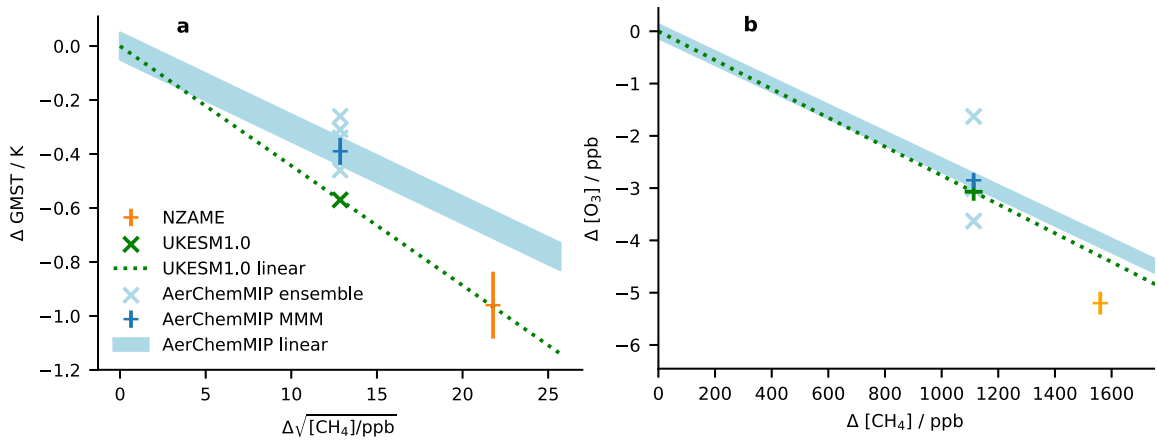

Fig. 4 Comparison of ZAME and AerChemMIP ozone and temperature changes with respect to methane concentration. AerChemMIP results are shown in blue, the UKESM ensemble member in green and ZAME in orange. Linear trends are extrapolated to test linearity of ZAME with respect to AerChemMIP. **a** Difference in global mean surface temperature (ΔGMST) vs the difference in square root of methane concentration ($\Delta\sqrt{[CH_4]}$) for 2015–2050, according to the relationship between methane concentration and radiative forcing[34]. **b** Difference in ozone concentration ($\Delta[O_3]$) vs difference in methane concentration ($\Delta[CH_4]$) between 2015 and 2050. Error bars represent the standard error.

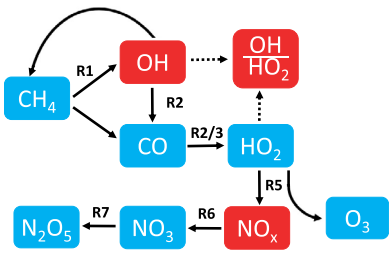

Fig. 5 Schematic of the relevant reactions linking methane, HOx and NOx. Species that decrease in ZAME are labelled in blue, and those that increase in red. Solid arrows represent reactions, with labels referencing the relevant reaction in the Methods section. The dashed arrows show how OH and HO_2 both contribute to the OH/HO_2 ratio. This is a simplified schematic of a more complex system that includes more feedbacks, such as between HOx, NOx and ozone.

emissions—rather than a lower boundary condition, as used by all the models in the AerChemMIP study[17] and the recent GMA study[8]. We suggest that UKCA-CH4 more faithfully simulates the O_3 response possible under extreme methane mitigation.

DISCUSSION

Methane plays a central role in the chemistry of the atmosphere. Through a cascade of chemical reactions (see 'Methods'), perturbations to methane affect many species and result in numerous feedbacks. The chemistry scheme in UKCA-CH4 allows us to model these effects.

Simple models of methane chemistry[35–37] fail to capture the effects of methane oxidation on HOx and NOx. Figure 5 shows the methane chemical cascade we simulate in UKCA-CH4. Under ZAME, the total methane emissions are reduced by ~60% (relative to 2015), decreasing methane concentrations globally. Methane is a source for secondary production of carbon monoxide (CO): this production is reduced, so the CO concentration decreases.

Reaction of CO with OH (reaction 2) is the main formation pathway for HO_2. The decrease in CO leads to less production of HO_2, and therefore lower modelled concentrations of HO_2. Reaction with CO and CH_4 (reactions 1 and 2) are the main sink pathways for OH. With both species depleted, the sink for OH decreases, leading to an increase in OH. The decrease in HO_2 and the increase in OH both contribute to increasing the OH/HO_2 ratio, which we see in ZAME increases by 16% by 2050 (see Supplementary Fig. 1).

The reduction in HO_2 slows production of O_3. By 2050, ozone in ZAME is much lower than in SSP3-7.0 (see Fig. 2d). The $HO_2 + NO$ reaction flux (the primary source of tropospheric ozone) (reaction 5) decreases (15 % by 2050) and so results in an ozone decrease. Secondly, the flux through the $HO_2 + O_3$ reaction increases (reaction 4), which depletes ozone. Both of these flux changes result in decreased ozone concentrations. Counter-intuitively, the $HO_2 + O_3$ flux increases despite decreases in both HO_2 and O_3. The origin of the drivers behind this have not been determined but will be the focus of future work.

Finally, we look at the response of NOx, which may be expected to be small, because NOx emissions are unchanged in ZAME. However, we find that the NOx concentrations are higher (Supplementary Fig. 2), which implies that the overall NOx lifetime has increased. The decrease in HO_2 means less NO is destroyed via reaction 5, so the NO increases. NO_3 is produced via the reaction of NO_2 with O_3. With less O_3, less NO_3 is produced and so the steady-state concentration of NO_3 is lower. NO_3 and NO_2 react together to form the reservoir species, N_2O_5 (reaction 7). With less NO_3, less N_2O_5 is produced, and this sink pathway for NO_2 is lower, resulting in higher NO_2 concentrations. Nitric acid (HNO_3), the other reservoir species for NOx, formed via reaction 8, increases slightly, but this reaction is very buffered and so large changes are not seen. Overall, these responses indicate a strong coupling between NOx and HOx in the model[38]. This makes attribution of the driving factors difficult in a small set of experiments, but it shows that there are strong feedbacks present that are not able to be represented in simpler models.

Although the methane emissions in ZAME are similar to pre-industrial levels, the burden equilibrates to levels significantly below these (Fig. 1). This reflects the very different atmospheric oxidising capacity simulated in ZAME (Fig. 2a). The oxidising capacity is mainly controlled by the amount of OH in the atmosphere, which is controlled by the balance of sources and sinks. OH is much higher in future scenarios than in the pre-industrial atmosphere, due to the reduction of the OH sinks (via CH_4 and CO) described above and an increase in water vapour (H_2O), which is a feedback of the future climate change. Increasing H_2O leads to an increase in the probability of $O(^1D)$

(formed from O_3) forming HOx. This in turn depletes more CH_4 and CO, leading to a further decrease in the OH sink.

We argue the change in methane burden reflects the state dependence of the methane self-feedback process. We capture these effects and the knock-on impacts more fully in our simulations: by including CH_4 emissions directly, and having a fully interactive chemistry scheme with HOx and NOx coupling (unlike simpler emission driven models e.g., Hayman et al.[19], Rigby et al.[36] and Turner et al.[37]). We argue that this self-feedback process is also not accurately simulated in surface concentration-driven methane models, including those that have participated in CMIP6 and sub-projects, like AerChemMIP[39] (which use an LBC). The strength of the self-feedback varies across the globe[38]. The interaction of the non-uniform methane emissions in UKCA-CH4 with areas of high and low feedback strength is more representative of the physical Earth system, compared to an LBC model, where the surface methane concentrations are globally invariant. Calculation of the LBC trajectory from emissions requires intermediate, lower complexity models, with assumptions about methane lifetime and therefore oxidising capacity. There is also a non-physical adjustment process at the lower boundary due to the fixed surface methane concentration. The climate feedbacks on natural methane sources are also not considered in these LBC projects[40], but are enabled here.

Failure to capture these feedbacks accurately will affect the atmospheric composition response to methane emissions changes. These emissions changes, with the self-feedback enabled, resulting in an increase in an oxidising capacity (see OH in Fig. 2a) that is simulated to be unprecedented over the last 150 years. By using the emissions-driven model, we avoid the use of an intermediate model, the non-physical adjustment process at the surface, and any effects on OH these have.

In summary, we have shown that with the cessation of anthropogenic methane emissions, the methane burden can decrease to below pre-industrial levels within 15 years. In the SSP3-7.0 scenario, 1° of future warming can be attributed, directly and indirectly, to the methane concentration change resulting from the anthropogenic methane emissions. Reduction in the methane source leads to large scale changes in atmospheric composition, increasing the oxidising capacity of the atmosphere to levels not seen in the last 150 years.

In the future zero anthropogenic methane emissions scenario, surface ozone concentrations are greatly reduced, showcasing the air-quality (and therefore human health) impacts of anthropogenic methane in the counterfactual scenario. We calculate ~690,000 premature deaths (due to ozone) per year by 2050 are attributable to anthropogenic methane in the SSP3-7.0 scenario. Given our use of the highest emissions scenario for ozone precursors (SSP3-7.0), our estimates for the climate and ozone changes attributable to future anthropogenic methane represent the upper bound of its impact.

Our work supports the growing literature of studies calculating significant co-benefits of methane action, such as the recent Global Methane Pledge. The use of methane emissions-driven Earth system models in follow-up studies is key to quantifying the full response of the Earth system to future methane changes, including the methane self-feedback and composition changes.

METHODS

UKCA-CH4 model configuration

The model version used here is derived from Version 1 of the UK Earth System Model (UKESM1) which has methane prescribed at the surface as a lower boundary condition (LBC)[33]. Land surface parameters and interactions are simulated using the Joint UK Land and Earth Surface model (JULES)[41]. In UKESM1, the methane wetland emissions are diagnosed in JULES but not coupled into the methane cycle. Atmospheric chemistry is simulated by the United Kingdom Chemistry and Aerosol Model (UKCA)[42].

UKCA-CH4, the model used in this experiment, is modified from UKESM1.0 to include a comprehensive representation of methane processes. This model includes surface emissions of methane instead of an LBC. The wetland methane emissions output by JULES couple into the model radiation and chemistry schemes, allowing for simulation of the climate feedback described by Gedney et al.[43]. Anthropogenic and biomass burning methane emissions used are from CMIP6 emissions datasets[23]. Predicted biomass burning and wetland emissions both have a high uncertainty associated with them[5]. The small proportion of natural methane emissions which arise from non-wetland sources, including ocean, geological and termite sources[44] are prescribed at 50 Tg per year and have no annual cycle. They are assumed to be constant over the whole model period since their magnitude and evolution over time is highly uncertain[45]. Methane surface deposition was also added in UKCA-CH4 to complete the representation of methane sources and sinks (reaction with OH, Cl, soil sink and stratospheric loss). Otherwise, UKCA-CH4 is identical to UKESM1.0 in terms of chemistry, Earth system and ocean dynamics.

ZAME experiment setup

SSP3-7.0 was used as our counterfactual scenario, the most extreme in terms of methane in CMIP6[23,46]. We instantaneously removed the anthropogenic methane emissions from 2015 onwards, leaving only wetland, biomass burning and non-wetland natural emissions (see Fig. 1a). The experiment was run with a fully coupled atmosphere-ocean at N96 resolution, from 2015 to 2050. Three ensemble members each were run for the counterfactual and ZAME scenarios, continuing from one of three different historical realisations. These are shown in the figures in a lighter colour, with the ensemble mean in the darker colour.

Data analysis

The methane surface concentrations were compared to observations from the National Oceanic and Atmospheric Administration Global Monitoring Laboratory (NOAA/GML), shown as black crosses in Fig. 1b (Dlugokencky, NOAA/GML, gml.noaa.gov/ccgg/trends_ch4/).

Global mean values are area-weighted means unless otherwise stated. Global mean airmass-weighted tropospheric OH was calculated using the method in Lawrence et al.[47]. The methane lifetime calculated here is the tropospheric methane lifetime due to reaction with OH: the whole atmosphere burden divided by the tropospheric CH_4-OH flux, according to the method in Voulgarakis et al.[48].

We used a linear fit to calculate the rate of temperature increase after 2035, with the value quoted as the mean gradient of the three ensemble members.

We calculated area-weighted and population-weighted mean surface ozone concentrations. The population data used from SSP1 and SSP3 were from Jones and O'Neill[28], for 2050.

Ozone mortality calculation

We calculated the mortality association with long-term ozone exposure according to the method in Malley et al.[30]. We used 2015 global average mortality data for cardiovascular and respiratory diseases from the Global Burden of Disease database[49] (http://ghdx.healthdata.org/gbd-results-tool), and the uncertainty limits quoted are derived from the uncertainty of the mortality rate. We used 2050 population estimates for SSP3 from Jones and O'Neill[28], and population age distribution data estimated by the UN population division for 2050 (https://population.un.org/wpp/DataQuery/). This is the same method as used in Shindell et al.[8], but we used global average mortality where they use country-specific mortality.

HOx/NOx coupling analysis

Below are the reactions relevant for understanding the HOx and NOx coupling and the impacts of methane on ozone.

$$CH_4 + OH \longrightarrow CH_3 + H_2O \quad (1)$$

$$CO + OH \longrightarrow CO_2 + H \quad (2)$$

$$H + O_2 + M \longrightarrow HO_2 + M \quad (3)$$

$$HO_2 + O_3 \longrightarrow OH + 2O_2 \quad (4)$$

$$HO_2 + NO \longrightarrow OH + NO_2 \quad (5)$$

$$NO_2 + O_3 \longrightarrow NO_3 + O_2 \quad (6)$$

$$NO_2 + NO_3 \longrightarrow N_2O_5 \quad (7)$$

$$NO_2 + OH \longrightarrow HNO_3 \quad (8)$$

DATA AVAILABILITY

UKCA-CH4 data used in this work are archived to the UK Centre for Environmental Data Analysis and are freely available[50]. Data sources used for ozone mortality calculations can be found in 'Methods'.

CODE AVAILABILITY

Code used for data analysis and producing figures can be found at https://github.com/zosiast/nzame-scripts.

Received: 27 August 2021; Accepted: 21 February 2022;
Published online: 23 March 2022

REFERENCES

1. UNFCCC. The Paris Agreement. https://unfccc.int/process-and-meetings/the-paris-agreement/the-paris-agreement (2015).
2. Pierrehumbert, R. T. Short-lived climate pollution. *Annu. Rev. Earth Planet Sci* **42**, 341–379 (2014).
3. IPCC. *Climate Change 2021: The Physical Science Basis. Contribution of Working Group I to the Sixth Assessment Report of the Intergovernmental Panel on Climate Change* (Cambridge University Press, 2021).
4. Nisbet, E. G. et al. Very strong atmospheric methane growth in the 4 years 2014–2017: Implications for the Paris agreement. *Global Biogeochem. Cy.* **33**, 318–342 (2019).
5. Saunois, M. et al. The global methane budget 2000–2017. *Earth Syst. Sci. Data* **12**, 1561–1623 (2020).
6. Shoemaker, J. K., Schrag, D. P., Molina, M. J. & Ramanathan, V. What role for short-lived climate pollutants in mitigation policy? *Science* **342**, 1323–1324 (2013).
7. Ocko, I. B. et al. Acting rapidly to deploy readily available methane mitigation measures by sector can immediately slow global warming. *Environ. Res. Lett.* **16**, 054042 (2021).
8. Shindell, D. et al. *Global Methane Assessment: Benefits and Costs of Mitigating Methane Emissions* (Nairobi: United Nations Environment Programme, 2021).
9. Harmsen, M. et al. The role of methane in future climate strategies: mitigation potentials and climate impacts. *Clim. Change* **163**, 1409–1425 (2020).
10. Shindell, D., Fuglestvedt, J. & Collins, W. The social cost of methane: theory and applications. *Faraday Discuss.* **200**, 429–451 (2017).
11. Nisbet, E. et al. Methane mitigation: methods to reduce emissions, on the path to the Paris agreement. *Rev. Geophys.* **58**, e2019RG000675 (2020).
12. Höglund-Isaksson, L., Gómez-Sanabria, A., Klimont, Z., Rafaj, P. & Schöpp, W. Technical potentials and costs for reducing global anthropogenic methane emissions in the 2050 timeframe–results from the GAINS model. *Environ. Res. Commun.* **2**, 025004 (2020).
13. Jackson, R. B. et al. Atmospheric methane removal: a research agenda. *Philos. Trans. Royal Soc. A* **379**, 20200454 (2021).
14. Boucher, O. & Folberth, G. A. New directions: atmospheric methane removal as a way to mitigate climate change? *Atmos. Environ.* **44**, 3343–3345 (2010).
15. Fiore, A. M., West, J. J., Horowitz, L. W., Naik, V. & Schwarzkopf, M. D. Characterizing the tropospheric ozone response to methane emission controls and the benefits to climate and air quality. *J. Geophys. Res. Atmos.* **113**, (2008).
16. Stohl, A. et al. Evaluating the climate and air quality impacts of short-lived pollutants. *Atmos. Chem. Phys.* **15**, 10529–10566 (2015).
17. Allen, R. J. et al. Significant climate benefits from near-term climate forcer mitigation in spite of aerosol reductions. *Environ. Res. Lett.* **16**, 034010 (2021).
18. Shindell, D. T., Faluvegi, G., Bell, N. & Schmidt, G. A. An emissions-based view of climate forcing by methane and tropospheric ozone. *Geophys. Res. Lett.* **32**, 1–4 (2005).
19. Hayman, G. D. et al. Regional variation in the effectiveness of methane-based and land-based climate mitigation options. *Earth Syst. Dynam.* **12**, 513–544 (2021).
20. Heimann, I. et al. Methane emissions in a chemistry-climate model: feedbacks and climate response. *J. Adv. Model. Earth Syst.* **12**, e2019MS002019 (2020).
21. Folberth, G. A. et al. Methane past, present and future-250-year methane trend from a fully interactive earth system model simulation. in *EGU General Assembly Conference Abstracts*, EGU2020–12808 (2020).
22. He, J., Naik, V., Horowitz, L. W., Dlugokencky, E. & Thoning, K. Investigation of the global methane budget over 1980–2017 using GFDL-AM4. 1. *Atmos. Chem. Phys.* **20**, 805–827 (2020).
23. Gidden, M. J. et al. Global emissions pathways under different socioeconomic scenarios for use in CMIP6: a dataset of harmonized emissions trajectories through the end of the century. *Geosci. Model Dev.* **12**, 1443–1475 (2019).
24. Abernethy, S., O'Connor, F., Jones, C. & Jackson, R. Methane removal and the proportional reductions in surface temperature and ozone. *Philos. Trans. Royal Soc. A* **379**, 20210104 (2021).
25. Archibald, A. et al. Tropospheric ozone assessment report: a critical review of changes in the tropospheric ozone burden and budget from 1850 to 2100. *Elementa Sci. Anthrop.* **8**, 1 (2020).
26. Naik, V. et al. Preindustrial to present-day changes in tropospheric hydroxyl radical and methane lifetime from the Atmospheric Chemistry and Climate Model Intercomparison Project (ACCMIP). *Atmos. Chem. Phys.* **13**, 5277–5298 (2013).
27. Stevenson, D. S. et al. Trends in global tropospheric hydroxyl radical and methane lifetime since 1850 from AerChemMIP. *Atmos. Chem. Phys.* **20**, 12905–12920 (2020).
28. Jones, B. & O'Neill, B. C. Spatially explicit global population scenarios consistent with the shared socioeconomic pathways. *Environ. Res. Lett.* **11**, 084003 (2016).
29. Griffiths, P. T. et al. Tropospheric ozone in CMIP6 simulations. *Atmos. Chem. Phys.* **21**, 4187–4218 (2021).
30. Malley, C. S. et al. Updated global estimates of respiratory mortality in adults ≥30 years of age attributable to long-term ozone exposure. *Environ. Health Perspect.* **125**, 087021 (2017).
31. O'Connor, F. M. et al. Assessment of pre-industrial to present-day anthropogenic climate forcing in UKESM1. *Atmos. Chem. Phys.* **21**, 1211–1243 (2021).
32. Shindell, D. et al. A climate policy pathway for near-and long-term benefits. *Science* **356**, 493–494 (2017).
33. Sellar, A. A. et al. UKESM1: description and evaluation of the U.K. earth system model. *J. Adv. Model. Earth Syst.* **11**, 4513–4558 (2019).
34. Etminan, M., Myhre, G., Highwood, E. & Shine, K. Radiative forcing of carbon dioxide, methane, and nitrous oxide: a significant revision of the methane radiative forcing. *Geophys. Res. Lett.* **43**, 12–614 (2016).
35. Prather, M. J. Lifetimes and time scales in atmospheric chemistry. *Philos. Trans. Royal Soc. A* **365**, 1705–1726 (2007).
36. Rigby, M. et al. Role of atmospheric oxidation in recent methane growth. *Proc. Natl Acad. Sci. USA* **114**, 5373–5377 (2017).
37. Turner, A. J., Frankenberg, C., Wennberg, P. O. & Jacob, D. J. Ambiguity in the causes for decadal trends in atmospheric methane and hydroxyl. *Proc. Natl Acad. Sci. USA* **114**, 5367–5372 (2017).
38. Holmes, C. D. Methane feedback on atmospheric chemistry: methods, models, and mechanisms. *J. Adv. Model. Earth Syst.* **10**, 1087–1099 (2018).
39. Collins, W. J. et al. Aerchemmip: quantifying the effects of chemistry and aerosols in cmip6. *Geosci. Model Dev.* **10**, 585–607 (2017).
40. Kleinen, T., Gromov, S., Steil, B. & Brovkin, V. Atmospheric methane underestimated in future climate projections. *Environ. Res. Lett.* **16**, 094006 (2021).
41. Clark, D. B. et al. The joint UK land environment simulator (JULES), model description—Part 2: carbon fluxes and vegetation dynamics. *Geosci. Model Dev.* **4**, 701–722 (2011).
42. Archibald, A. T. et al. Description and evaluation of the UKCA stratosphere–troposphere chemistry scheme (StratTrop vn 1.0) implemented in UKESM1. *Geosci. Model Dev.* **13**, 1223–1266 (2020).
43. Gedney, N., Huntingford, C., Comyn-Platt, E. & Wiltshire, A. Significant feedbacks of wetland methane release on climate change and the causes of their uncertainty. *Environ. Res. Lett.* **14**, 084027 (2019).
44. Fung, I. et al. Three-dimensional model synthesis of the global methane cycle. *J. Geophys. Res.* **96**, 13033–13065 (1991).

45. Etiope, G., Schwietzke, S., Helmig, D. & Palmer, P. Global geological methane emissions: an update of top-down and bottom-up estimates. *Elementa Sci. Anthrop*. **7**, (2019).
46. O'Neill, B.C. et al. The Scenario Model Intercomparison Project (ScenarioMIP) for CMIP6. *Geosci. Model Dev*. **9**, 3461–3482 (2016).
47. Lawrence, M., Jöckel, P. & Kuhlmann, R. V. What does the global mean oh concentration tell us? *Atmos. Chem. Phys* **1**, 37–49 (2001).
48. Voulgarakis, A. et al. Sciences ess Atmospheric chemistry and physics climate of the past geoscientific instrumentation methods and data systems analysis of present day and future OH and methane lifetime in the ACCMIP simulations. *Atmos. Chem. Phys* **13**, 2563–2587 (2013).
49. Murray, C. J. et al. Global burden of 87 risk factors in 204 countries and territories, 1990–2019: a systematic analysis for the global burden of disease study 2019. *Lancet* **396**, 1223–1249 (2020).
50. Staniaszek, Z. et al. UKCA-CH4 output for methane emissions-driven and methane LBC-driven future climate projections under SSP3-7.0 and SSP1-2.6 scenarios. NERC EDS Centre for Environmental Data Analysis. https://doi.org/10.5285/d1c277836e754e279c9a964ad3d95828 (2021).

ACKNOWLEDGEMENTS

The use of UKESM1.0 was facilitated by the use of the Monsoon2/NEXCS system, a collaborative facility supplied under the Joint Weather and Climate Research Programme, a strategic partnership between the Met Office and the Natural Environment Research Council. This work used JASMIN, the UK collaborative data analysis facility. Z.S. was supported by the UKRI NERC C-CLEAR DTP, grant reference number: NE/S007164/1. P.T.G. and A.T.A. were supported by the UKRI NERC National Centre for Atmospheric Science. For the development of the methane emissions-driven configuration, used here, G.A.F. and F.M.O'C. were supported by the Met Office Hadley Centre Climate Programme funded by BEIS and Defra (grant no. GA1101).

AUTHOR CONTRIBUTIONS

Z.S. designed the study, analysed the results and wrote the manuscript, in discussion with A.T.A. and P.T.G. at all stages. A.T.A. contributed to writing the manuscript. N.L.A. helped set up and run the experiments. G.A.F. and F.M.O'C. developed and provided the underlying UKCA-CH4 model. All authors reviewed the manuscript.

COMPETING INTERESTS

The authors declare no competing interests.

ADDITIONAL INFORMATION

Supplementary information The online version contains supplementary material available at https://doi.org/10.1038/s41612-022-00247-5.

Correspondence and requests for materials should be addressed to Zosia Staniaszek or Alexander T. Archibald.

Reprints and permission information is available at http://www.nature.com/reprints

Publisher's note Springer Nature remains neutral with regard to jurisdictional claims in published maps and institutional affiliations.

Open Access This article is licensed under a Creative Commons Attribution 4.0 International License, which permits use, sharing, adaptation, distribution and reproduction in any medium or format, as long as you give appropriate credit to the original author(s) and the source, provide a link to the Creative Commons license, and indicate if changes were made. The images or other third party material in this article are included in the article's Creative Commons license, unless indicated otherwise in a credit line to the material. If material is not included in the article's Creative Commons license and your intended use is not permitted by statutory regulation or exceeds the permitted use, you will need to obtain permission directly from the copyright holder. To view a copy of this license, visit http://creativecommons.org/licenses/by/4.0/.

© The Author(s) 2022